Biol Blood Marrow Transplant 25 (2019) 1911–1919

Biology of Blood and Marrow Transplantation

journal homepage: www.bbmt.org

Biology

IL-22 Accelerates Thymus Regeneration via Stat3/Mcl-1 and Decreases Chronic Graft-versus-Host Disease in Mice after Allotransplants

Bin Pan[1,2], Dong Wang[1], Lingling Li[1], Longmei Shang[1], Fan Xia[1], Fan Zhang[1], Ying Zhang[3], Robert Peter Gale[4], Mengdi Xu[1,2], Zhenyu Li[1,2], Kailin Xu[1,2,*]

[1] *Blood Diseases Institute, Xuzhou Medical University, Xuzhou, China*
[2] *Department of Hematology, The Affiliated Hospital of Xuzhou Medical University, Xuzhou Medical University, Xuzhou, China*
[3] *Department of Pathology, Xuzhou Medical University, Xuzhou, China*
[4] *Centre for Haematology Research, Division of Experimental Medicine, Department of Medicine, Imperial College London, London, United Kingdom*

Article history:
Received 13 February 2019
Accepted 2 June 2019

Keywords:
IL-22
Thymus
Thymic epithelial cell
Graft-versus-host disease

A B S T R A C T

High-dose chemotherapy and/or radiation given before an allogeneic hematopoietic cell transplantation severely damage thymic epithelial cells (TECs), resulting in poor post-transplant immune recovery. IL-22 mediates recovery of TECs via a proregenerative effect, but the precise mechanism by which this occurs is unknown. In this study, we found IL-22 improved thymus recovery after damage from irradiation in association with increased number of TECs. This effect was blocked by ruxolitinib, a *JAK1/JAK2* inhibitor. IL-22 increased the number of TECs via a Stat3-dependent signaling in the mTEC1 murine thymic epithelial cell line. This, in turn, upregulated transcription of myeloid cell leukemia sequence 1 (*Mcl1*), resulting in increased number of TECs. Similar effects were seen in irradiated mice given IL-22. Defects in IL-22 resulted in delayed thymus recovery in irradiated mice and had an impact on levels of thymus function-related genes such as *Foxn1, Aire*, and *Kgf*. In mice, post-transplant use of IL-22 improved repair of TECs, increased the numbers of thymus T cells, increased the intrathymic levels of Aire, and increased the proportion of natural regulatory T cells, resulting in decreased severity of chronic graft-versus-host disease (GVHD). Our data highlight the critical role of the IL-22/Stat3/Mcl-1 pathway in the regeneration of TECs after damage from irradiation in mice and highlight circumstances where normalizing thymus T cell function with IL-22 decreases GVHD after allotransplants.

INTRODUCTION

Thymic epithelial cells (TECs) are important for T cell development [1]. The thymus is very sensitive to stress such as infection, anticancer chemotherapy, and ionizing radiation [2]. Thymus dysfunction decreases T cell immunity, predisposing patients to infection and autoimmune diseases [3,4]. Because TECs are critical for differentiation and survival of thymocytes, improving recovery of TECs after pretransplant conditioning is a potential strategy to reconstitute T cell immunity following hematopoietic cell transplantation [5].

IL-22 is a member of the IL-10 family of cytokines, which mediate inflammation and regulate epithelial cell homeostasis [6,7]. Therapy with recombinant human IL-22 is being tested in persons with hepatitis (NCT02655510) and gastrointestinal graft-versus-host disease (GVHD; NCT02406651). IL-22 was recently reported to accelerate recovery of TECs after allogeneic hematopoietic cell transplantation in mice [8,9]. We reported upregulation of intrathymic IL-22 correlated with thymus regeneration in mice exposed to total-body radiation (TBI). Loss of CD4 and CD8 double-positive thymocytes may trigger upregulation of intrathymic IL-22 levels [10].

The Janus kinase/signal transducer of activators of transcription (JAK/STAT) signaling pathway is important in transducing signals from the IL-22 receptor [7]. Activation of Stat3 regulates proliferation and regeneration of epithelial cells [11,12]. However, it is unclear how Stat3 regulates proliferation of TECs.

We reported that IL-22-producing T cells are involved in the pathogenesis of acute GVHD in mice [13]. IL-22 has pro- and anti-inflammatory effects in different experimental scenarios [7]. Because of the important role of IL-22 in epithelial cell homeostasis, we interrogated how IL-22 mediates thymus regeneration after allotransplant in mice. We found IL-22 mediates thymus regeneration by increasing the number of TECs via

Financial disclosure: See Acknowledgments on page 1918.
* Correspondence and reprint requests: Kailin Xu, MD, Department of Hematology, The Affiliated Hospital of Xuzhou Medical University, Xuzhou Medical University, 99 West Huaihai Road, Xuzhou 221002, China.
E-mail address: lihmd@163.com (K. Xu).

https://doi.org/10.1016/j.bbmt.2019.06.002
1083-8791/

a JAK/Stat3/myeloid cell leukemia sequence 1 (Mcl-1) pathway after injury induced by irradiation and that IL-22 improves thymus and T cell recovery in murine allotransplants.

METHODS

Mice

Wild-type (WT) BALB/c and C57BL/6 mice were purchased from Charles River (Vital River, Beijing, China). IL-22 knockout (IL-22KO) mice with a C57BL/6 background were obtained from Cyagen Biosciences (Suzhou, China). IL-22KO mice were generated by using transcription activator-like effector nuclease (Cyagen Biosciences, Suzhou, China). Mice were bred in a special pathogen-free room. Procedures regarding animal care and experiments were approved by the Experimental Animal Care and Use Committee of Xuzhou Medical University.

Cell Culture

The murine thymic epithelial cell line mTEC1, kindly provided by Prof. Yu Zhang (Peking University, Beijing) [14], was cultured in DMEM (Thermo Fisher Scientific, Waltham, MA) medium supplied with 10% FBS (Biowest, Nuaillé, France).

Reagents

Recombinant murine IL-22 (rmIL-22) was purchased from PeproTech (210-22; Rocky Hill, NJ). Ruxolitinib, fludarabine, stattic, napabucasin, ABT-737, and A-1210477 were purchased from ApexBio (Houston, TX). STAT5-IN-1 was obtained from MedChemExpress (Shanghai, China).

Thymic Injury Model

To induce thymus injury, 6-week-old WT or IL-22KO mice were exposed to 5.5 Gy TBI from a ^{137}Cs source (Gamma-Service Medical GmbH, Leipzig, Germany) at a dose rate of 0.65 Gy/min. Mice were injected intraperitoneally with PBS or rmIL-22 (0.1 mg/kg) on days 0, 2, 4, 6, and 8 following TBI. Some mice received ruxolitinib (90 mg/kg, gavage) or stattic (3 mg/kg, i.p. injection) on days 0, 2, 4, 6, and 8 following TBI.

Bone Marrow Transplant Models

Bone marrow transplants were done as described [15]. Eight-week-old mice were used. In the C57BL/6 → BALB/c model, BALB/c recipients received 7.5 Gy TBI followed by an infusion of 5 × 10E+6 T cell-depleted (TCD) bone marrow cells from a C57BL/6 donor. Then, 5 × 10E+5 T cells from a C57BL/6 donor were coinfused to induce acute and chronic GVHD. In the BALB/c → C57BL/6 model, C57BL/6 recipients received 9.0 Gy TBI followed by an infusion of 5 × 10E+6 TCD bone marrow cells and 5 × 10E+5 T cells from a BALB/c donor. Recipients were injected intraperitoneally with PBS or rmIL-22 (0.1 mg/kg) on days 0, 2, 4, 6, and 8 post-transplant.

Assessment of GVHD

Severity of systemic GVHD was assessed by 5 clinical scores as reported [16]. Chronic skin GVHD was scored based on histology, including cell infiltration, fat loss, dermal fibrosis, and epidermal interface changes after hematoxylin and eosin (H&E) and Masson staining [17].

Masson Staining and H&E Staining

Masson staining was performed on paraffin slides of skin tissues with a Trichrome Stain Kit (HT15; Sigma-Aldrich, Shanghai, China). H&E staining was performed on paraffin slides as described [15].

Thymic Stroma Cell Isolation

Thymic stroma cells were isolated as described [10]. Briefly, a freshly dissected thymus was cut into small pieces, mechanically dissociated in DMEM containing 2% FBS, and centrifuged at 400 × g. Pellets were twice digested with 0.5 mg/mL collagenase type IV (Thermo Fisher Scientific) and 1 mg/mL DNase I (Sigma-Aldrich) for 30 minutes at 37°C and then a third time with 1 mg/mL Dispase (Sigma-Aldrich) for 5 minutes at 37°C. Cells were collected and suspended in PBS with 2% FBS and 5 mM EDTA.

Flow Cytometry and Cell Sorting

Thymus cells were stained with anti-CD45 (30-F11), anti-EpCAM (G8.8), anti-CD4 (RM4-5), anti-CD8a (53-6.7), and antilineage antigen. The lineage antigen cocktail contains anti-CD3e (145-2C11), anti-Gr-1 (RB6-8C5), anti-B220 (RA3-6B2), anti-TER119 (TER-119), anti-NK1.1 (PK136), and anti-CD11b (M1/70). Samples prepared from whole blood were stained with anti-CD45 (30-F11), anti-CD3e (145-2C11), anti-CD19 (6D5), anti-CD4 (RM4-5), anti-CD44 (IM7), anti-CD25 (3C7), and CD62L (MEL-14).

To analyze Th1 cells, spleen cells were processed using intracellular cytokine staining. Briefly, cells were stimulated with PMA (Sigma-Aldrich) and ionomycin (Sigma-Aldrich) in the presence of Brefeldin A (BD Biosciences, San Jose, CA) for 4 hours, followed by treatment with a Fixation/Permeabilization Solution Kit (BD Biosciences). Cells were stained with the following antibodies: anti-CD45 (30-F11), anti-CD3e (145-2C11), anti-CD4 (RM4-5), and anti-IFN-γ (XMG1.2). CD45$^+$CD3$^+$CD4$^+$IFN-γ^+ cells were defined as Th1 cells. To analyze regulatory T cells (Tregs), cells were processed using a Foxp3/Transcription Factor Staining Buffer (eBioscience, Thermo Fisher Scientific). Cells were stained with the following antibodies: anti-CD45 (30-F11), anti-CD3e (145-2C11), anti-CD4 (RM4-5), anti-FoxP3 (FJK-16s), and anti-neuropilin-1 (3DS304M). CD3$^+$CD4$^+$FoxP3$^+$ cells were defined as Tregs. Neuropilin-1$^+$ Tregs were defined as natural Tregs (nTregs), and neuropilin-1$^-$ Tregs were defined as induced Tregs [18]. To analyze IL-22-producing cells, thymus cells were processed with a Foxp3/Transcription Factor Staining Buffer as described. Cells were stained with the following antibodies: anti-CD45 (30-F11), anti-CD3e (145-2C11), anti-F4/80 (T45-2342), anti-CD4 (RM4-5), anti-IL-7Rα (SB/199), anti-RORγt (Q31-378), and anti-IL-22 (Poly5164).

To detect incorporation of EdU in TECs, mice were injected intraperitoneally with 0.1 mg EdU. Thymii were collected after 24 hours, and a single-cell suspension was prepared. Cells were stained with anti-CD45 (30-F11) and anti-EpCAM (G8.8) and then processed with an EdU Flow Cytometry Assay Kit (A007; GeneCopoeia, Guangzhou, China) following the manufacturer's instructions.

Apoptosis was quantified by staining with an annexin V/propidium iodide apoptosis detection kit (556547; BD Biosciences). Antibodies were purchased from eBioscience (Thermo Fisher Scientific), BD Biosciences, or BioLegend (San Diego, CA). Cells were analyzed on an LSRFortessa flow cytometer (BD Biosciences). TECs were sorted on an Influx cell sorter (BD Biosciences).

ELISA

Thymii from mice were mildly ground in 1 mL PBS and the supernatant collected. IL-22 concentrations in thymus supernatants and plasma from mice were quantified using a mouse IL-22 ELISA kit (Thermo Fisher Scientific).

Cytometry Bead Array

Plasma concentrations of IL-2, IL-4, IL-10, IL-6, IL-17A, IFN-γ, and TNF-α were measured with a cytometry bead array (CBA) kit (560485; BD Biosciences).

Quantitative PCR

Total RNA isolation and cDNA synthesis were performed as described [15]. cDNA concentrations were analyzed by quantitative PCR (qPCR) with a LightCycler 480 SYBR Green I Master qRT-PCR kit (Roche, Mannheim, Germany). Glyceraldehyde-3-phosphate dehydrogenase (*Gapdh*) transcript levels were used for normalization. Results were analyzed by $-\Delta\Delta C_T$ values. These primers were synthesized from Thermo Fisher Scientific: *Il22* (TCGCCTTGATCTCTCCACTC and GCTCAGCTCCTGTCACATCA), *Foxn1* (GCCGACCTGCTTCACTGAG and GTGGAGCCTGGAAGTGTGA), *Aire* (GACTCCAGGTCGTCCCTATG and GAAGCTGTACCCACCTCTGG), *Kgf* (GAGAG-GCTCAAGTTGCACGA and CGGTTGCTCCTTGACTTTTGT), *Mcl1* (GGCCAAA-CACTTAAAGAGCG and TGGAAGAACTCCACAAACCC), *Il21* (CACATAGCTAA-ATGCCCTTCCTGT and ATCATCTGTGGGAACGAGAGC), *Igf1* (CCTGCCTGGGT-GTCCAAATG and ATGTGTATCTTTATTGCAGGTGCG), *Gh* (ATAAAAAGGG-CACGCAAGGG and AGGAGGTCCGAGAGTCTGTAG), *Ccl25* (GTAACCCAGGCAG-CAGTCTT and AAACTGTGGCTTTTTGCCTG), *Dll4* (TATAACCCTTTGGCCCA-CTG and ATGGGGAGGTCTGTTTTGTG), *Il7* (CACATCATCTGAGTGCCACA and GTTTGGTTCATTATTCGGGC), *Il12* (TGCATCTGGCGTCTACACTG and GCCAAAAA-GAGGAGGTAGCGT), and *Gapdh* (TTGATGGCAACAATCTCCAC and CGTCCCGT-AGACAAAATGGT). qPCR was performed on an LC480 cycler (Roche).

Cell Viability Assay

Cell viability was measured with a Cell Counting Kit-8 (CCK-8, CK04) from DOJINDO (Tokyo, Japan).

Western Blotting

Cell proteins were extracted by using Cell Lysis Buffer (Cell Signaling Technology, Danvers, MA). Western blot analyses were done with the following antibodies: Phospho-STAT3 (Tyr705), STAT3, Phospho-STAT5 (Tyr694), STAT5, Phospho-STAT1 (Tyr701), STAT1, Phospho-ERK (T202/Y204), ERK, Phospho-p38 (Thr180/Tyr182), p38, Mcl-1 (D2W9E), Bcl-2 (D17C4), Bcl-xL (54H6), Bim (C34C5), Bak (D4E4), and GAPDH (D16H11) purchased from Cell Signaling Technology. Anti-AIRE (orb216017) was purchased from Biorbyt (Cambridge, United Kingdom).

RNA Interference

Mcl1-targeting small interfering RNAs (siRNAs) (*Mcl1* siRNA-1: GCAG-GAUUGUGACUCUUAU, *Mcl1* siRNA-2: GCGUAAACCAAGAAAGCUU, *Mcl1* siRNA-3: GGACUGGCUUGUCAAACAA) and *Stat3*-targeting siRNAs (*Stat3* siRNA-1: UUCUUAAUUUGUUGGCGGG, *Stat3* siRNA-2: UGUUAAAUUUCCGA-GACCC, *Stat3* siRNA-3: ACUUUCCAAAUGCCUCCUC), synthesized from Genecreate (Wuhan, China), were transfected into mTEC1 cells using HiPerFect Transfection Reagent (QIAGEN, Shanghai, China). Preliminary experiments identified *Mcl1* siRNA-3 as the most efficient for silencing *Mcl1* transcription, which was downregulated by 71%. An irrelevant siRNA (Genecreate) was used as a control.

Overexpression of Mcl-1

Coding sequence fragment (996 bp) of mouse *Mcl1* (NM_008562.3) was synthesized and cloned to pCDH-CMV-MCS-EF1-GFP-Puro lentiviral vector (Genecreate). Lentiviral particles were produced by transfecting 293FT cells with the Mcl-1 overexpression lentiviral vector, which was packed in a ViraPower HiPerform Lentiviral Expression System (Invitrogen, Thermo Fisher Scientific). mTEC1 cells, stably expressing Mcl-1 overexpression vector, were obtained by transducing cells with lentiviral particles followed by selection with puromycin. A blank vector was used as control.

Chromatin immunoprecipitation

Chromatin immunoprecipitation assay was performed with an Enzymatic Chromatin IP Kit (9003; Cell Signaling Technology). Briefly, formaldehyde-fixed cells were lysed. Nuclei were collected and chromatin fragmented by enzymatic digestion. Chromatin fragments were immunoprecipitated by anti-STAT3 (4904; Cell Signaling Technology) or normal rabbit immunoglobulin G. DNA was purified from the precipitated chromatin. Standard PCR (35 cycles) and qPCR (40 cycles) were used to identify promoter regions of *Fos* and *Mcl1* genes. The following primers were used in PCR: *Fos* (TCACTTGCTGCTTCCAACCT and GAGAAGCAAGTACGCAGCCT) and *Mcl1* (CAGCAGGTAGTGCAACGAGA and CCTGCTGATCTGTGTCGGTT). Enrichment of a specific DNA fragment was expressed as signal relative to input based on results from qPCR testing.

Immune Histochemistry

Immune histochemistry was performed on paraffin slides of the thymii to detect Aire expression. Anti-AIRE (orb135062) was from Biorbyt (Cambridge, United Kingdom). Peroxidase-conjugated goat anti-rabbit IgG (ZSGB-BIO, Beijing, China) was used as a second antibody. 3,3′-Diaminobenzidine substrate was used for visualization (ZSGB-BIO).

Statistics

Survival was compared using a log-rank test. Data were presented as mean ± SD. Comparisons of means were performed with an unpaired Student *t* test or 1-way analysis of variance test with Bonferroni correction. *P* values $<.05$ were considered significant.

RESULTS

Defects in IL-22 Levels Delayed Regeneration of Thymus after Damage from Irradiation

To evaluate the dynamics of IL-22 production in sublethally irradiated mice, we prepared supernatants from thymii and tested these for IL-22 concentration by ELISA. IL-22 concentrations increased from days 1 to 7 postradiation and then returned to baseline. IL-22-producing cells were analyzed in thymii of the irradiated mice. Most IL-22-producing cells were group 3 innate lymphoid cells (ILC3s). T cells and macrophages produced small amounts of IL-22. Intraperitoneal injection of rmIL-22 increased the IL-22 concentration in damaged thymii (Supplemental Figure S1) and accelerated thymus recovery as indicated by increased numbers of thymocytes and TECs. Injection of rmIL-22 also increased T cell levels in the blood. Increased numbers of thymocytes were attributed to CD4 and CD8 double-positive (DP) and to CD4 or CD8 single-positive (SP) thymocytes with no significant change in levels of CD4 and CD8 double-negative thymocytes (Figure 1A,B).

We next studied the effects of rmIL-22 on IL-22KO mice. Untreated IL-22KO mice have the same size thymus and numbers of TECs as WT mice (Supplemental Figure S2). Irradiated IL-22KO mice had delayed recovery of thymus cell numbers and TECs compared with WT mice. This effect was reversed by intraperitoneal injection of rmIL-22 into IL-22KO mice (Figure 1C). TECs of IL-22KO mice had a decreased level of phosphorylated Stat3, an effect reversed by injection of rmIL-22 (Figure 1D).

We also analyzed expression levels of messenger RNA (mRNA) of several thymus functional genes in TECs from irradiated mice [1]. IL-22KO mice had reduced expression levels of forkhead box N1 (*Foxn1*), autoimmune regulator (*Aire*), and keratinocyte growth factor (*Kgf*) (Supplemental Figure S3). These data suggest IL-22 regulates regeneration of TECs after damage from ionizing radiation.

IL-22 Increased Number of TECs and Stat3/Mcl-1 Signaling

Because injection of rmIL-22 increased numbers of TECs in thymii exposed to ionizing radiation, we tested if IL-22 regulated growth of mTEC1 cells, a murine thymic epithelial cell line. rmIL-22 exposure increased the number of mTEC1 cells (Figure 2A). IL-22/IL-22R transduces signaling through the JAK/STAT and mitogen-activated kinase-like protein (MAPK) pathways [19]. IL-22 exposure increased phosphorylation of Stat3, Stat5, and extracellular signal-regulated kinase (ERK) in mTEC1 cells. In contrast, IL-22 exposure did not activate the Stat1 and p38 signaling pathways (Figure 2B). To test whether the JAK/STAT pathway might be an intracellular target of IL-22, we added ruxolitinib to mTEC1 cultures. Ruxolitinib addition strongly decreased the number of mTEC1 cells with or without IL-22 and reduced phosphorylation of Stat1, Stat3, and Stat5 but not ERK and p38 (Figure 2B-D). Because Stat1, Stat3, and Stat5 are important mediators of epithelial cell proliferation [8,19], we used the Stat1 inhibitor fludarabine, the Stat3 inhibitor stattic, and the Stat5 inhibitor STAT5-IN-1 to block activation. Stattic decreased the number of mTEC1 strongly, whereas fludarabine and STAT5-IN-1 were less effective (Figure 2E). Growth of mTEC1 could also be significantly suppressed by another Stat3 inhibitor, napabucasin, and by knockdown of *Stat3* expression with siRNAs (Supplemental Figure S4). Like ruxolitinib, stattic blocked IL-22-induced growth of mTEC1 (Figure 2F).

Because Stat3 inhibitors induced significant apoptosis of mTEC1 cells (Figure 3A and Supplemental Figure S4), we analyzed expression of some apoptosis-related proteins. Stattic reduced the levels of phospho-Stat3 and Mcl-1 (Figure 3B). In contrast, ruxolitinib-treated mTEC1 cells had decreased levels of Bcl-2, Bcl-xL, and BIM levels, which were unchanged in stattic-treated cells. STAT5-IN-1 treatment reduced levels of Bcl-2 and Bcl-xL but had no effect on BIM levels. No inhibitor altered BAK levels (Figure 3B).

We tested whether antiapoptotic proteins of the Bcl-2 family had an impact on growth of mTEC1 using selective inhibitors A-1210477 and ABT-737 for blocking Mcl-1 and Bcl-2/Bcl-xL. A-1210477 decreased the number of mTEC1 cells more efficiently than ABT-737 (Figure 3C). Next, we studied whether IL-22 regulated *Mcl1* transcript levels. IL-22 treatment increased *Mcl1* transcript levels in mTEC1 cells (Figure 3D). Using chromatin immunoprecipitation, we found Stat3 binds the promoter region of *Mcl1* in mTEC1 cells, an effect blocked by stattic treatment (Figure 3E,F). Knockdown of *Mcl1* expression with siRNAs reversed growth-promoting effects of IL-22 on mTEC1 cells (Figure 3G), whereas overexpression of *Mcl1* counteracted stattic-induced growth suppression of mTEC1 cells (Figure 3H). These data indicate IL-22 increases the number mTEC1 via the Stat3/Mcl-1 pathway.

Because of the role of the JAK/STAT signaling pathway in regulating growth of TECs, we tested effects of ruxolitinib and stattic on thymus recovery in irradiated mice. Ruxolitinib-treated mice had smaller thymii and decreased numbers of thymus cells, TECs, and blood T cells compared with controls (Figure 4A,B). Ruxolitinib treatment also reduced expression levels of intrathymic phospho-Stat3 and Mcl-1 (Figure 4C). Stattic showed a similar effect on recovery of thymus cells in irradiated mice (Supplemental Figure S5).

Injection of rmIL-22 Accelerated T Cell Reconstitution in Mice after Allotransplant

Next, we tested whether giving IL-22 improved T cell reconstitution in irradiated mice receiving an allotransplant. In the C57BL/6 → BALB/c model, C57BL/6 and BALB/c mice were

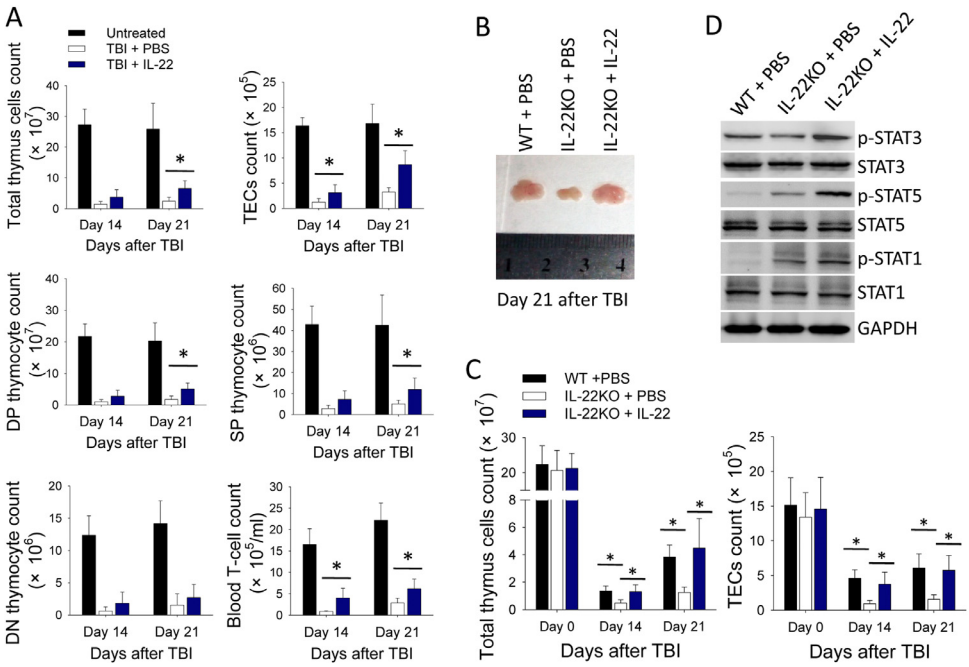

Figure 1. IL-22-mediated thymus regeneration after injury. (A) WT C57BL/6 mice were exposed to 5.5 Gy TBI. Mice received PBS or IL-22 (0.1 mg/kg) on days 0, 2, 4, 6, and 8. Thymus and blood samples were obtained after TBI (n = 5). Flow cytometry was applied to analyze proportions of TECs, DP, SP, and double-negative (DN) thymocytes in total thymus cells. Blood T cells were also analyzed. (B-D) WT and IL-22KO mice were exposed to 5.5 Gy TBI. IL-22KO mice were injected with PBS or IL-22 (0.1 mg/kg) on days 0, 2, 4, 6, and 8. (B) A representative photo displays thymus size from each cohort (n = 4). (C) Total thymus cells were counted and TECs were measured by flow cytometry (n = 4). (D) Thymic stromal cells were prepared from thymus on day 14 after TBI. TECs were sorted from thymic stromal cells. Total cell proteins were extracted and subjected to Western blot analysis with antibodies indicated. The experiment was repeated twice. Data are shown as mean ± SD, compared using an unpaired *t* test or a 1-way analysis of variance test. $^*p < .05$.

used as donors and recipients, respectively (Figure 5A and Supplemental Figure S6A). Injection of rmIL-22 accelerated thymus recovery indicated by more thymus cells, TECs, and DP and SP thymocytes (Figure 5A). Injection of rmIL-22 increased levels of blood T cells and CD4-positive, CD25-negative, CD44-negative, and CD62L-positive T cells (naive T cells), an indicator

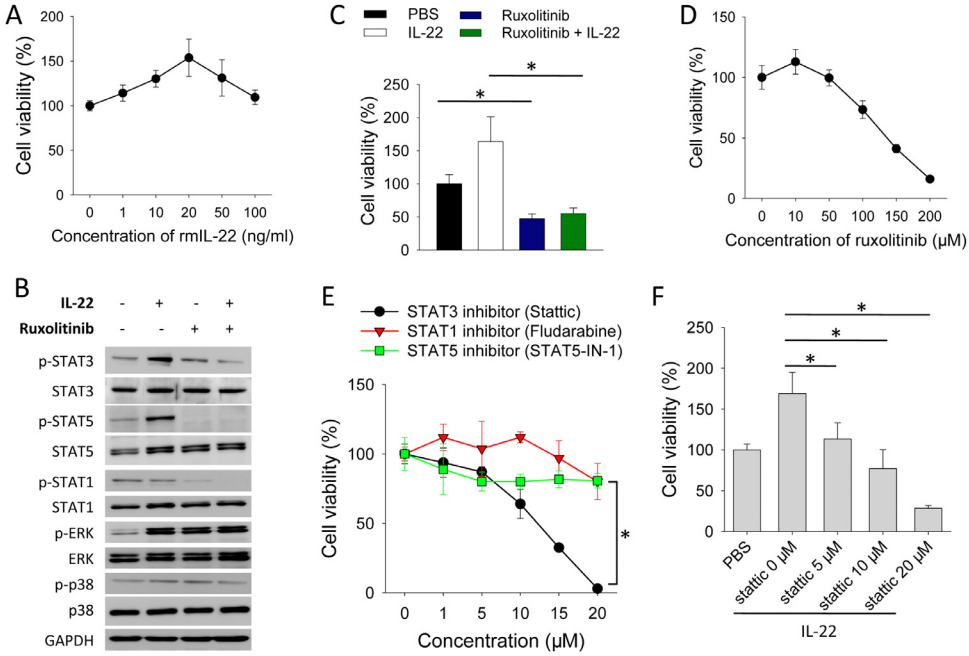

Figure 2. IL-22 increased number of TECs in a Stat3-dependent manner. (A) Murine thymic epithelial cells (mTEC1) were cultured with different doses of rmIL-22 for 24 hours. Cell viability was measured by the CCK-8 assay (n = 6). (B, C) mTEC1 cells were cultured in the presence of IL-22 (20 ng/mL) with or without ruxolitinib (100 μM) for 24 hours. (B) Total cell proteins were extracted and subjected to Western blot analysis with antibodies indicated. The experiment was repeated 3 times. (C) Cell viability was measured by the CCK-8 assay (n = 6). (D, E) mTEC1 cells were cultured with different doses of ruxolitinib, stattic, fludarabine, or STAT5-IN-1 for 24 hours. Cell viability was measured by the CCK-8 assay (n = 6). (F) mTEC1 cells were cultured with different doses of stattic in the presence of IL-22 (20 ng/mL) for 24 hours. Cell viability was measured by the CCK-8 assay (n = 6). Data are mean ± SD, compared using 1-way analysis of variance test. $^*p < .05$.

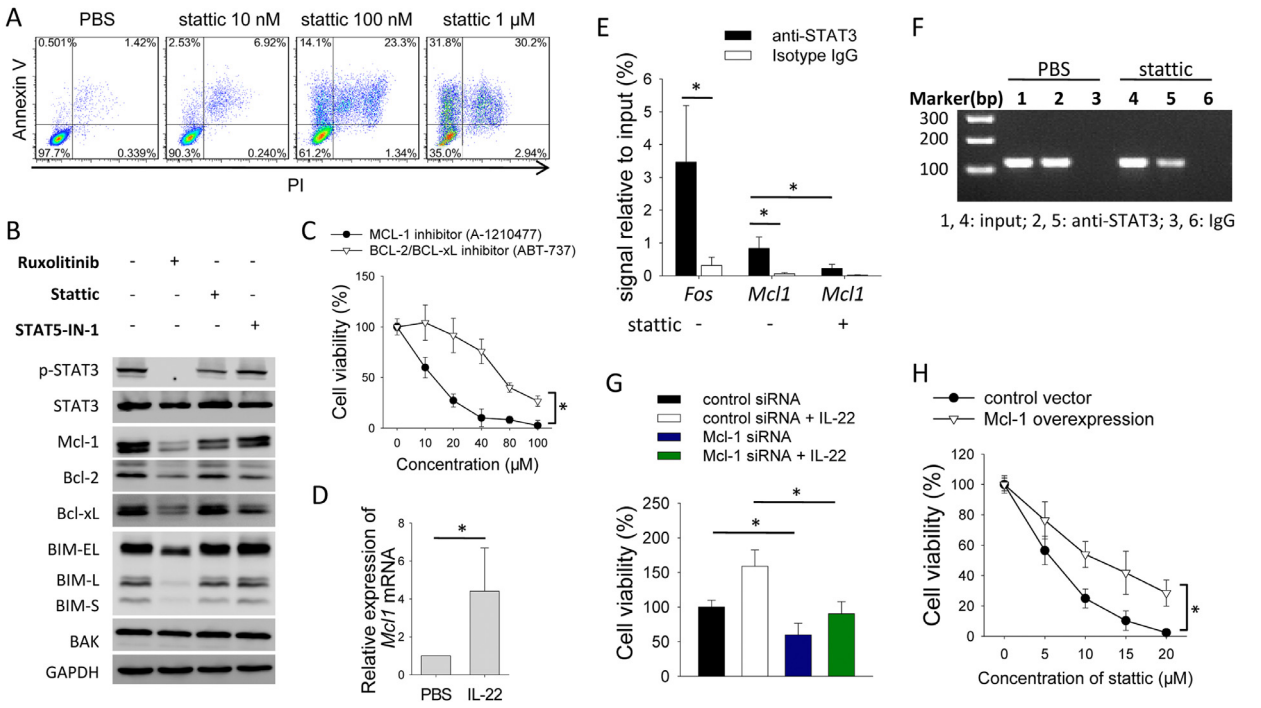

Figure 3. Mcl-1 mediated the growth-promoting effect of IL-22 in mTEC1 cells. (A) mTEC1 cells were cultured with stattic for 96 hours. Apoptosis was analyzed by flow cytometry. Annexin-V$^+$PI$^-$ population indicated early apoptotic cells, and annexin-V$^+$PI$^+$ population indicated late apoptotic cells. PI, propidium iodide. (B) mTEC1 cells were cultured with ruxolitinib (100 μM), stattic (10 μM), or STAT5-IN-1 (10 μM) for 24 hours. Total cell proteins were analyzed by Western blot with antibodies indicated. BIM-EL, BIM-L, and BIM-S are 3 alternative splicing isoforms of BIM. The experiment was repeated 3 times. (C) mTEC1 cells were cultured with A-1210477 or ABT-737 for 48 hours. Cell viability was measured by the CCK-8 assay (n = 6). (D) mTEC1 cells were cultured with IL-22 (20 ng/mL) for 24 hours. Expression of *Mcl1* mRNA was measured by qPCR (n = 6). (E, F) mTEC1 cells were cultured with or without stattic (10 μM) for 24 hours. Cells were subjected to chromatin immunoprecipitation (ChIP) analysis. Chromatin fragments were immunoprecipitated by anti-Stat3 or isotype immunoglobulin G. DNA was purified from the precipitated chromatin. (E) qPCR and (F) standard PCR were used to detect promoter region of the *Mcl1* gene, with *Fos* as a positive control gene. Enrichment of a specific DNA fragment was expressed as signal relative to input based on C_T values from qPCR. Signal relative to input = $2\% \times 2^{[CT\ (2\%\ Input)\ -\ CT\ (ChIP)]}$. The experiment was repeated 3 times. (G, H) mTEC1 cells were transfected with *Mcl1* siRNA or negative control siRNA, followed by culture with IL-22 (20 ng/mL) for 24 hours (G). mTEC1 cells, stably expressing a Mcl-1 overexpression vector, were treated with stattic for 24 hours (H). Cell viability was measured by the CCK-8 assay (n = 6). Data are shown as mean ± SD, compared using an unpaired *t* test or a 1-way analysis of variance test. $^*p < .05$.

of recent thymic emigrants [20], on days 14 and 21 post-transplant compared with controls (Figure 5A). In contrast to other thymocytes, rmIL-22 treatment increased the number of CD4 and CD8 double-negative thymocytes on day 14 but not on day 21 (Figure 5A). There was no significant change in numbers of blood B cells (Figure 5A). Injection of rmIL-22 stimulated proliferation of TECs and increased the intrathymic levels of *Mcl1* mRNA (Supplemental Figure S6B,C). Injection of rmIL-22 showed a similar effect on T cell reconstitution in the BALB/c → C57BL/6 model (Figure 5B).

IL-22 Increased Levels of Intrathymic Tregs and Reduced Skin Chronic GVHD after Allotransplant

Next, we analyzed effects of IL-22 injection on GVHD in mice. There was no effect on acute GVHD scores or survival compared with controls except for a transient increase in IL-17A plasma levels on day 7 post-transplant (Supplemental Figure S7). In contrast, rmIL-22-treated mice had lower systemic GVHD scores, lower skin chronic GVHD scores, and less skin cell infiltration and collagen deposition on day 60 post-transplant (Figure 6A-C). Levels of intrathymic Aire were increased in rmIL-22-treated mice (Figure 6D,E). Injection of rmIL-22 decreased levels of Th1 but increased levels of neuropilin-1-positive Tregs (nTregs) [18] in spleen (Figure 6F). Injection of rmIL-22 also increased levels of nTregs in thymus. IL-22 had no impact on levels of induced Tregs in spleen or thymus (Figure 6F). Injection of rmIL-22 reduced plasma level of IFN-γ on day 60 post-transplant (Figure 6G).

DISCUSSION

We found IL-22 is important for thymus regeneration after damage from irradiation. IL-22 had a growth-promoting effect on murine TECs in a Stat3/Mcl-1-dependent manner. Exogenous IL-22 improved thymus regeneration in murine allotransplant recipients and reduced severity of chronic skin GVHD (Figure 7).

TECs provide growth signals to developing thymocytes. Consequently, promoting TEC recovery is a promising strategy to accelerate thymus reconstitution after injury. Previous studies reported that KGF, IL-7, growth hormone, insulin-like growth factor 1 and IL-22 accelerated thymus recovery [8,9,21-24]. We found that levels of IL-22 in the thymus and plasma increased after thymus injury induced by irradiation. Because intrathymic supernatants contain both extracellular fluid and intrathymic blood plasma, increased levels of intrathymic IL-22 might derive from extracellular fluid, intrathymic blood, or both. We cannot precisely identify the source (s). ILC3s was a major cellular source of IL-22 in thymus of the irradiated mice. IL-22KO mice have defective thymus regeneration after injury induced by irradiation, which is reversed by exogenous IL-22. IL-22KO mice show more severe thymus dysfunction indicated by the reduced intrathymic transcript levels of *Foxn1*, *Aire*, and *Kgf* after injury. Foxn1 is a key regulator of thymic development in the embryonic and postnatal periods [25]. Aire mediates a negative selection function of the thymus [26]. KGF is thought to mediate regeneration of TECs [27].

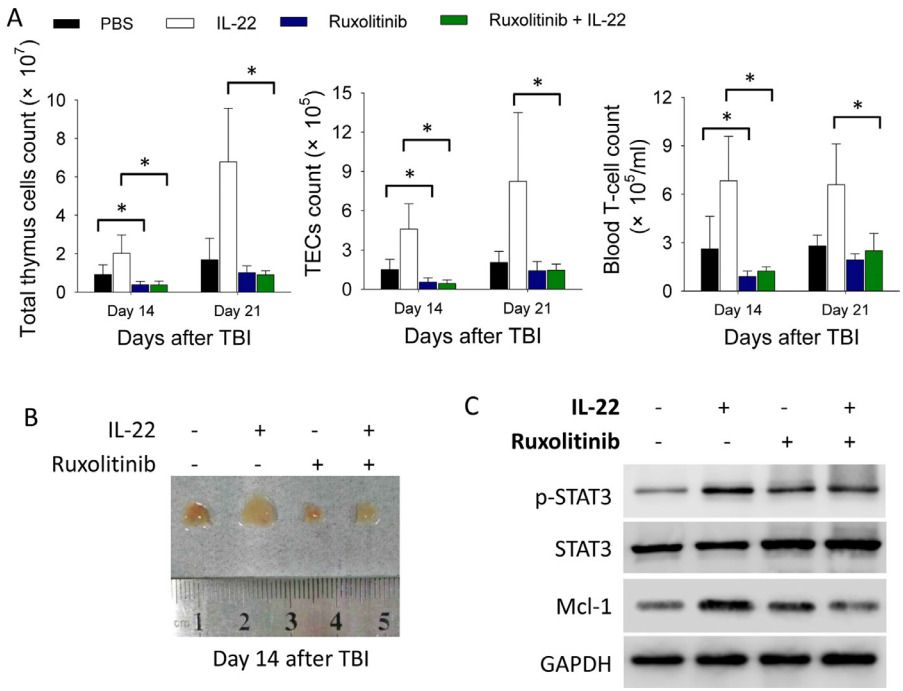

Figure 4. Ruxolitinib blocked the proregenerative effect of IL-22 on injured thymus. WT C57BL/6 mice were exposed to 5.5 Gy TBI. Mice received IL-22 (0.1 mg/kg) with or without ruxolitinib (90 mg/kg) on days 0, 2, 4, 6, and 8. (A) Flow cytometry was used to analyze numbers of TECs and blood T cells (n = 5). (B) A representative photo displays thymus size from each cohort (n = 3). (C) Thymic stromal cells were prepared on day 21 after TBI (n = 3). Total cell proteins were extracted and subjected to Western blot analysis with the antibodies indicated. The experiment was repeated 3 times. Data are mean ± SD, compared using a 1-way analysis of variance test. $^{*}p < .05$.

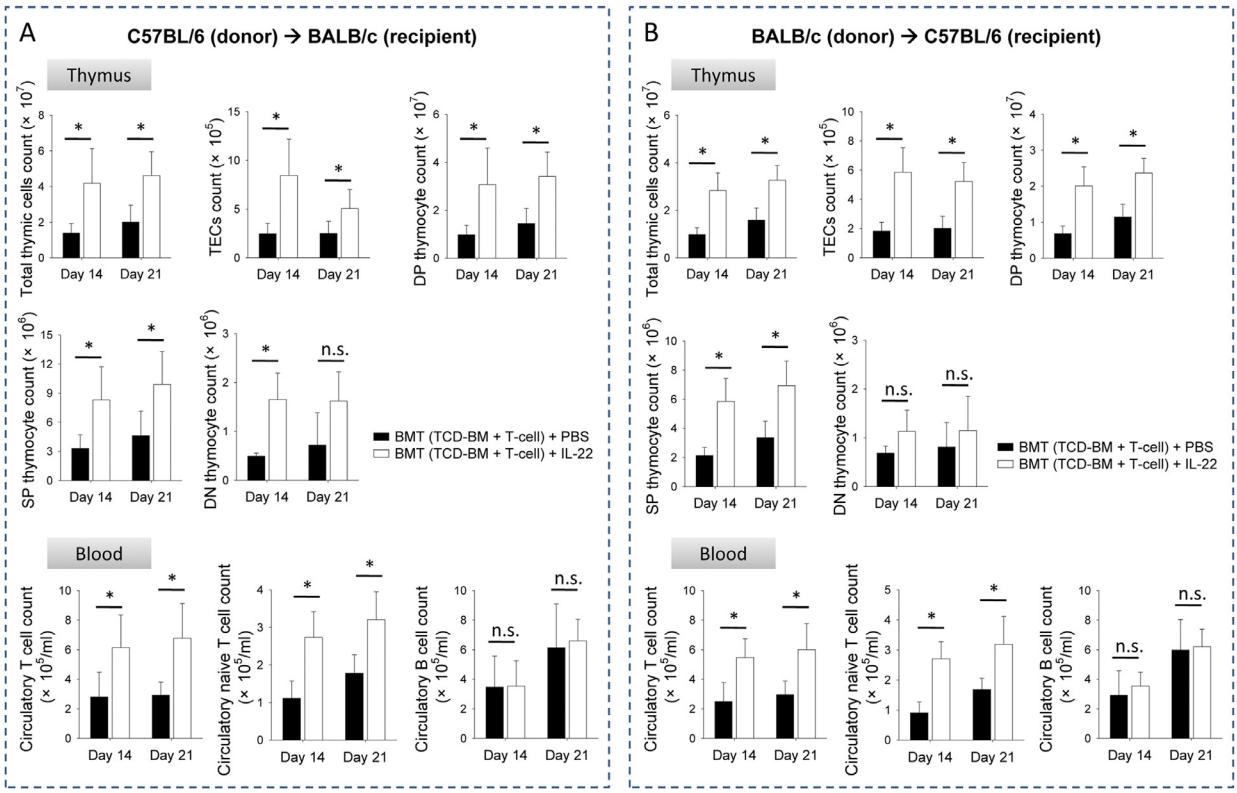

Figure 5. Exogenous IL-22 accelerated reconstitution of T cells in murine allogeneic bone marrow transplants (allo-BMTs). In C57BL/6 (donor) → BALB/c (recipient) allo-BMT (A) and BALB/c (donor) → C57BL/6 (recipient) allo-BMT (B) models, irradiated recipients were infused with T cell-depleted bone marrow cells and splenic T cells from donor. Recipients received PBS or rmIL-22 (0.1 mg/kg) on days 0, 2, 4, 6, and 8. Thymus and blood samples were obtained. Flow cytometry was applied to analyze numbers of TECs, DP thymocytes, SP thymocytes, double-negative thymocytes, blood T cells, blood B cells, and blood naive T cells (n = 5). The $CD44^{-}CD62L^{+}$ population was defined as naive T cells after gating on $CD4^{+}CD25^{-}$ T cells. Data are mean ± SD, compared using an unpaired *t* test. $^{*}p < .05$; n.s., no significance.

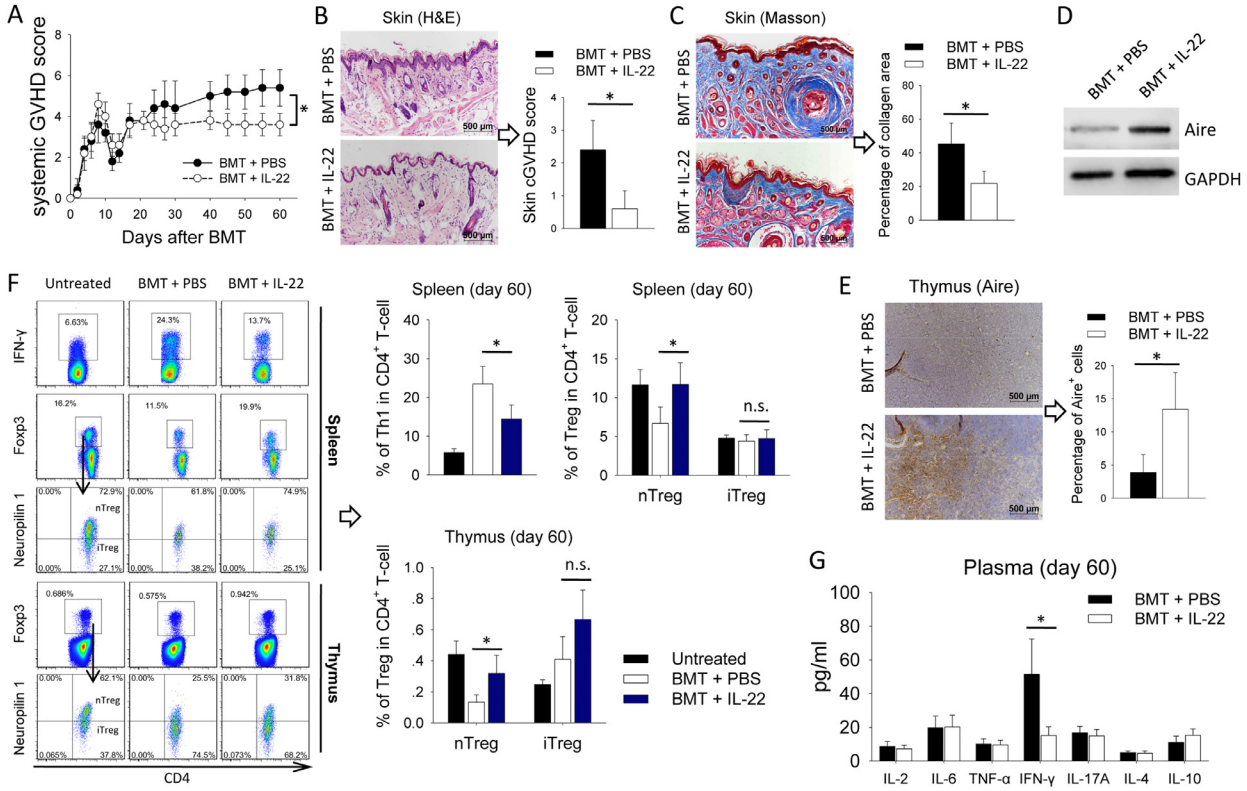

Figure 6. Exogenous IL-22 decreased skin chronic GVHD in mice. In the C57BL/6 → BALB/c model, irradiated recipients received an allotransplant. Recipients received PBS or rmIL-22 (0.1 mg/kg) on days 0, 2, 4, 6, and 8. (A) Systemic GVHD score was monitored continuously (n = 5). Samples were obtained on day 60 post-transplant. H&E staining (B) and Masson staining (C) were performed on paraffin slides of skin tissues (n = 3). Skin chronic GVHD was scored as described. Collagen deposit, visualized by Masson staining, was quantified by percentage of collagen area measured by ImageJ software. (D) Total protein was extracted from thymus and subjected to Western blot analysis with antibodies indicated. The experiment was repeated 3 times. (E) Expression of Aire in thymus was detected by immunohistochemistry (n = 3). Percentage of Aire$^+$ cells was counted. Scale bar (B, C, E): 500 μm. (F) Flow cytometry was applied to analyze percentages of Th1 and Treg cells in spleen and thymus (n = 4). Neuropilin 1-positive Treg was considered nTreg, and neuropilin 1-negative Treg was considered induced Treg (iTreg). (G) Plasma samples were subjected to cytometric bead array (CBA) analysis for levels of cytokines (n = 4). Data are mean ± SD, compared using an unpaired *t* test or a 1-way analysis of variance test. $^*p < .05$; n.s., no significance.

We identified a Stat3/Mcl-1 pathway through which IL-22 increased the number of TECs. Dudakov et al. [8] reported that IL-22 activates Stat1, Stat3, and Stat5. Our data indicate that Stat3 is most important in maintaining growth of TECs. Others reported that Stat3 signaling is required for survival of medullary TECs and maintenance of thymopoiesis [28], but it is unclear how this operates. Stat3 is a transcription factor that activates several downstream genes, including Bcl-2 family members [29]. We found Stat3 binds the promoter region of *Mcl1* and that IL-22 regulates growth of TECs via Mcl-1. Mcl-1, a member of the Bcl-2 family, is an antiapoptotic gene regulating survival of hematopoietic cells [30]. Stat3 also regulates expression of Bcl-2 and Bcl-xL in other cell types [31]. However, in murine TEC cells, Stat3 signaling had no significant impact on expression of Bcl-2 and Bcl-xL indicated by our Bcl-2 inhibitor data. A recent study by Jain et al. [32] also identified Mcl-1 as a critical regulator for development and survival of TECs. However, in contrast to our findings, Jain et al.[32] reported that epidermal growth factor upregulates Mcl-1 via a MAPK/ERK pathway. These data suggest Mcl-1 might be a common point shared by the JAK/STAT and MAPK/ERK pathways in TECs. TECs, especially the medullary compartment, have a high rate of proliferation and death. The balance between proliferation and apoptosis controls homeostasis of TECs [1,33]. Injection of IL-22 increased proliferation of TECs and intrathymic levels of *Mcl1* mRNA. Preconditioning of allogeneic hematopoietic cell transplantation induced severe damage of TECs. Mcl-1 is an antiapoptotic protein, which might protect TECs by inhibiting apoptosis. Also, STAT3 is a versatile transcriptional factor with the potential to upregulate other genes involved in the proliferation of epithelial cells.

Exogenous rmIL-22 stimulated proliferation of TECs in mouse allotransplant recipients, which, in turn, accelerated recovery of CD4 and CD8 DP and CD4 or CD8 SP thymocytes. Exogenous rmIL-22 increased levels of blood naive and total T cells but not total B cells. This may seem paradoxical given the decreased severity of chronic GVHD. However, rmIL-22 increased levels of intrathymic Aire, which might improve negative selection in the thymus and prevent release of autoreactive T cells, which might underlie some aspects of GVHD [26]. rmIL-22 also increased the level of intrathymic nTregs, which are important in maintaining immune tolerance [34]. These effects, alone or combined, may explain why the severity of chronic GVHD was reduced. Other data support the notion of less GVHD when there is better thymus function such as the lower incidence of GVHD in children compared with adults [35].

Others have reported both proinflammatory and anti-inflammatory functions of IL-22 in GVHD [36]. We recently reported an anti-inflammatory function of recipient antigen-presenting cells derived IL-22 from mice with acute GVHD [37]. Interestingly, recipient macrophage-derived Stat3 exerts an anti-GVHD effect [38]. Previous studies mostly focused on the direct immune regulatory role of IL-22. We show a

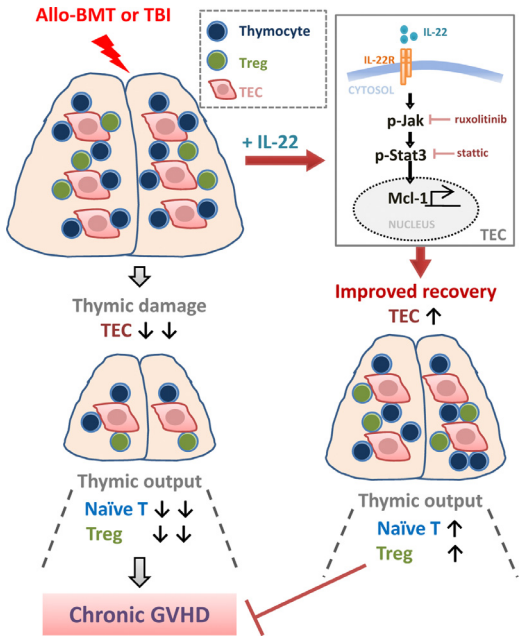

Figure 7. Proposed models of IL-22-mediated thymus recovery after an allotransplant. Pretransplant drugs and/or radiation severely damage thymus function, which results in decreased output of naive and regulatory T cells predisposing to chronic GVHD. Post-transplant use of IL-22 increases TEC numbers via the Stat3/Mcl-1 pathway, which accelerates thymus recovery. Use of IL-22 increases the level of thymus-derived nTregs and decreases skin chronic GVHD.

probable indirect immune regulatory role of IL-22, which functions by promoting recovery of damaged TECs.

Ruxolitinib reduced the number of TECs in a thymus damaged by irradiation that was associated with delayed T cell recovery. This effect could explain the immune suppression reported in persons with myeloproliferative neoplasm-associated myelofibrosis receiving ruxolitinib. A recent study reported that use of ruxolitinib caused more severe cytopenia in children, who in general have better thymus function compared with adults [39]. This relationship could be important as ruxolitinib was recently approved to treat acute GVHD in humans [40,41].

In conclusion, we show IL-22 increases the numbers of TECs and accelerates thymus recovery after damage from irradiation. This effect is mediated via the Stat3/Mcl-1 pathway. IL-22 improves thymus and T cell recovery in irradiated mice receiving an allotransplant and reduces the severity of chronic skin GVHD. These findings may have implications for human transplant recipients.

ACKNOWLEDGMENTS

Prof. Grzegorz Przybylski (Polish Academy of Medical Science) kindly reviewed the manuscript and provided helpful suggestions.

Financial disclosure: This study was supported by grants from the National Natural Science Foundation of China (81671584, 81871263, 81300377, 81570183, and 81500088), Natural Science Foundation of Jiangsu Province (BE2015625, BK20151153, and BK20161178), and Postdoctoral Science Foundation of Jiangsu Province (1601096B). R.P.G. acknowledges support from the National Institute for Health Research Biomedical Research Centre funding scheme.

Conflict of interest statement: R.P.G. is a part-time employee of Celgene Corp.

Authorship statement: K.X. contributed to the concept and design, analyzed data, and revised the manuscript. B.P. performed experiments, analyzed data, wrote the manuscript, and helped to design experiments. D.W. and L.L. performed experiments and analyzed data (bone marrow transplant model, constructing vector, and histopathology). L.S., F.X., F.Z., Y.Z., and M.X. performed part of experiments. Z.L. provided experimental expertise. R.P.G. advised on experimental design and revised the manuscript. B.P., D.W., and L.L. contributed equally to this study.

SUPPLEMENTARY MATERIALS

Supplementary material associated with this article can be found in the online version at doi:10.1016/j.bbmt.2019.06.002.

REFERENCES

1. Abramson J, Anderson G. Thymic epithelial cells. *Annu Rev Immunol*. 2017;35:85-118.
2. Gruver AL, Sempowski GD. Cytokines, leptin, and stress-induced thymic atrophy. *J Leukoc Biol*. 2008;84:915-923.
3. Bunting MD, Comerford I, Seach N, et al. CCX-CKR deficiency alters thymic stroma impairing thymocyte development and promoting autoimmunity. *Blood*. 2013;121:118-128.
4. Dertschnig S, Hauri-Hohl MM, Vollmer M, Hollander GA, Krenger W. Impaired thymic expression of tissue-restricted antigens licenses the de novo generation of autoreactive CD4+ T cells in acute GVHD. *Blood*. 2015;125:2720-2723.
5. Chaudhry MS, Velardi E, Malard F, van den Brink MR. Immune reconstitution after allogeneic hematopoietic stem cell transplantation: time to T up the thymus. *J Immunol*. 2017;198:40-46.
6. Zhao D, Kim YH, Jeong S, et al. Survival signal REG3-alpha prevents crypt apoptosis to control acute gastrointestinal graft-versus-host disease. *J Clin Invest*. 2018;128(11):4790-4797.
7. Dudakov JA, Hanash AM, van den Brink MR. Interleukin-22: immunobiology and pathology. *Annu Rev Immunol*. 2015;33:747-785.
8. Dudakov JA, Hanash AM, Jenq RR, et al. Interleukin-22 drives endogenous thymic regeneration in mice. *Science*. 2012;336:91-95.
9. Dudakov JA, Mertelsmann AM, O'Connor MH, et al. Loss of thymic innate lymphoid cells leads to impaired thymopoiesis in experimental graft-versus-host disease. *Blood*. 2017;130:933-942.
10. Pan B, Liu J, Zhang Y, et al. Acute ablation of DP thymocytes induces up-regulation of IL-22 and Foxn1 in TECs. *Clin Immunol*. 2014;150:101-108.
11. Pickert G, Neufert C, Leppkes M, et al. STAT3 links IL-22 signaling in intestinal epithelial cells to mucosal wound healing. *J Exp Med*. 2009;206:1465-1472.
12. Lindemans CA, Calafiore M, Mertelsmann AM, et al. Interleukin-22 promotes intestinal-stem-cell-mediated epithelial regeneration. *Nature*. 2015;528:560-564.
13. Zhao K, Zhao D, Huang D, et al. The identification and characteristics of IL-22-producing T cells in acute graft-versus-host disease following allogeneic bone marrow transplantation. *Immunobiology*. 2013;218:1505-1513.
14. Li J, Li Y, Yao JY, et al. Developmental pathway of CD4+CD8− medullary thymocytes during mouse ontogeny and its defect in Aire−/− mice. *Proc Natl Acad Sci U S A*. 2007;104:18175-18180.
15. Pan B, Wang X, Kojima S, et al. The fifth epidermal growth factor-like region of thrombomodulin alleviates murine graft-versus-host disease in a G-protein coupled receptor 15 dependent manner. *Biol Blood Marrow Transplant*. 2017;23:746-756.
16. Cooke KR, Kobzik L, Martin TR, et al. An experimental model of idiopathic pneumonia syndrome after bone marrow transplantation: I. The roles of minor H antigens and endotoxin. *Blood*. 1996;88:3230-3239.
17. Yamakawa T, Ohigashi H, Hashimoto D, et al. Vitamin A-coupled liposomes containing siRNA against HSP47 ameliorate skin fibrosis in chronic graft-versus-host disease. *Blood*. 2018;131(13):1476-1485.
18. Yadav M, Louvet C, Davini D, et al. Neuropilin-1 distinguishes natural and inducible regulatory T cells among regulatory T cell subsets in vivo. *J Exp Med*. 2012;209:1713-1722.
19. Ouyang W, Rutz S, Crellin NK, Valdez PA, Hymowitz SG. Regulation and functions of the IL-10 family of cytokines in inflammation and disease. *Annu Rev Immunol*. 2011;29:71-109.
20. Krenger W, Blazar BR, Hollander GA. Thymic T-cell development in allogeneic stem cell transplantation. *Blood*. 2011;117:6768-6776.
21. Rossi SW, Jeker LT, Ueno T, et al. Keratinocyte growth factor (KGF) enhances postnatal T-cell development via enhancements in proliferation and function of thymic epithelial cells. *Blood*. 2007;109:3803-3811.
22. Mackall CL, Fry TJ, Gress RE. Harnessing the biology of IL-7 for therapeutic application. *Nat Rev Immunol*. 2011;11:330-342.
23. Chen BJ, Cui X, Sempowski GD, Chao NJ. Growth hormone accelerates immune recovery following allogeneic T-cell-depleted bone marrow transplantation in mice. *Exp Hematol*. 2003;31:953-958.

24. Alpdogan O, Muriglan SJ, Kappel BJ, et al. Insulin-like growth factor-I enhances lymphoid and myeloid reconstitution after allogeneic bone marrow transplantation. *Transplantation*. 2003;75:1977-1983.
25. Zuklys S, Handel A, Zhanybekova S, et al. Foxn1 regulates key target genes essential for T cell development in postnatal thymic epithelial cells. *Nat Immunol*. 2016;17:1206-1215.
26. Malchow S, Leventhal DS, Lee V, Nishi S, Socci ND, Savage PA. Aire enforces immune tolerance by directing autoreactive T cells into the regulatory T cell lineage. *Immunity*. 2016;44:1102-1113.
27. Dooley J, Erickson M, Larochelle WJ, Gillard GO, Farr AG. FGFR2IIIb signaling regulates thymic epithelial differentiation. *Dev Dyn*. 2007;236:3459-3471.
28. Lomada D, Jain M, Bolner M, et al. Stat3 signaling promotes survival and maintenance of medullary thymic epithelial cells. *PLoS Genet*. 2016;12:e1005777.
29. Yue P, Lopez-Tapia F, Paladino D, et al. Hydroxamic acid and benzoic acid-based STAT3 inhibitors suppress human glioma and breast cancer phenotypes in vitro and in vivo. *Cancer Res*. 2016;76:652-663.
30. Opferman JT. Life and death during hematopoietic differentiation. *Curr Opin Immunol*. 2007;19:497-502.
31. Durant L, Watford WT, Ramos HL, et al. Diverse targets of the transcription factor STAT3 contribute to T cell pathogenicity and homeostasis. *Immunity*. 2010;32:605-615.
32. Jain R, Sheridan JM, Policheni A, et al. A critical epithelial survival axis regulated by MCL-1 maintains thymic function in mice. *Blood*. 2017;130:2504-2515.
33. Gray D, Abramson J, Benoist C, Mathis D. Proliferative arrest and rapid turnover of thymic epithelial cells expressing Aire. *J Exp Med*. 2007;204:2521-2528.
34. Blazar BR, MacDonald KPA, Hill GR. Immune regulatory cell infusion for graft-versus-host disease prevention and therapy. *Blood*. 2018;131:2651-2660.
35. Duncan CN, Majhail NS, Brazauskas R, et al. Long-term survival and late effects among one-year survivors of second allogeneic hematopoietic cell transplantation for relapsed acute leukemia and myelodysplastic syndromes. *Biol Blood Marrow Transplant*. 2015;21:151-158.
36. Lamarthee B, Malard F, Saas P, Mohty M, Gaugler B. Interleukin-22 in graft-versus-host disease after allogeneic stem cell transplantation. *Front Immunol*. 2016;7:148.
37. Pan B, Xia F, Wu Y, et al. Recipient-derived IL-22 alleviates murine acute graft-versus-host disease in association with reduced activation of antigen presenting cells. *Cytokine*. 2018;111:33-40.
38. Nieves EC, Toubai T, Peltier DC, et al. STAT3 expression in host myeloid cells controls graft-versus-host disease severity. *Biol Blood Marrow Transplant*. 2017;23:1622-1630.
39. Khandelwal P, Teusink-Cross A, Davies SM, et al. Ruxolitinib as salvage therapy in steroid-refractory acute graft-versus-host disease in pediatric hematopoietic stem cell transplant patients. *Biol Blood Marrow Transplant*. 2017;23:1122-1127.
40. von Bubnoff N, Ihorst G, Grishina O, et al. Ruxolitinib in GvHD (RIG) study: a multicenter, randomized phase 2 trial to determine the response rate of Rruxolitinib and best available treatment (BAT) versus BAT in steroid-refractory acute graft-versus-host disease (aGvHD) (NCT02396628). *BMC Cancer*. 2018;18:1132.
41. Gonzalez Vicent M, Molina B, Gonzalez de Pablo J, Castillo A, Diaz M.A. Ruxolitinib treatment for steroid refractory acute and chronic graft vs host disease in children: Cclinical and immunological results. *Am J Hematol*. 2019;94:319-326.